Ocean Sci. Discuss., 11, 3003–3034, 2014
www.ocean-sci-discuss.net/11/3003/2014/
doi:10.5194/osd-11-3003-2014

Ocean Science
Discussions
Open Access

In situ autonomous optical radiometry measurements for satellite ocean color validation in the Western Black Sea

G. Zibordi, F. Mélin, J.-F. Berthon, and M. Talone

European Commission, Joint Research Centre, Ispra, Italy

Received: 4 November 2014 – Accepted: 28 November 2014 – Published: 20 December 2014

Correspondence to: G. Zibordi (giuseppe.zibordi@jrc.ec.europa.eu)

Published by Copernicus Publications on behalf of the European Geosciences Union.

Abstract

The accuracy of primary satellite ocean color data products from the Moderate Resolution Imaging Spectroradiometer on-board Aqua (MODIS-A) and the Visible/Infrared Imager/Radiometer Suite (VIIRS), is investigated in the Western Black Sea using in situ measurements from the Gloria site included in the Ocean Color component of the Aerosol Robotic Network (AERONET-OC). The analysis is also extended to an additional well-established AERONET-OC site in the northern Adriatic Sea characterized by optically complex coastal waters exhibiting similarities with those observed at the Gloria site. Results from the comparison of normalized-water leaving radiance L_{WN} indicate biases of a few percent between satellite derived and in situ data at the center-wavelengths relevant for the determination of chlorophyll *a* concentration (443–547 nm, or equivalent). Remarkable is the consistency among the annual cycle determined with time series of satellite-derived and in situ L_{WN} ratios at these center-wavelengths. Contrarily, the differences between in situ and satellite-derived L_{WN} are pronounced at the blue (i.e., 412 nm) and red (i.e., 667 nm, or equivalent) center-wavelengths, suggesting difficulties in confidently applying satellite-derived radiometric data from these spectral regions for quantitative analysis in optically complex waters.

1 Introduction

During the last decades satellite ocean color data were applied to biology, biogeochemistry and climate change studies. For instance, time-series of chlorophyll *a* concentration (Chl *a*) were shown relevant: (i) to determine seasonal cycles of phytoplankton biomass and investigate the climate effects on marine ecosystems (Behrenfeld et al., 2006); (ii) to quantify primary production at regional and global scales (Longhurst et al., 1995, Field et al., 1998); (iii) to support studies on ecological processes (Platt et al., 2003), carbon cycle and air–sea fluxes (Lohrenz et al., 2006); and (iv) to sustain fishery services and coastal management (Stumpf, 2001; Ware and Thompson, 2005).

Confidence on remote sensing applications is established by the quality of satellite data products. Because of this, the assessment of satellite data is a major task of any ocean color mission performed by investigating uncertainties of primary (e.g., normalized water-leaving radiance) and derived (e.g., Chl *a*) data products through in situ reference data representative of the variety of observation conditions offered by the world seas. This is pursued by combining in situ data from different and often independent sources. However, data sets constructed following such a scheme are affected by overall uncertainties difficult to quantify because of the use of different instruments, measurement protocols, processing and quality assurance schemes. Thus, standardization of measurements through the application of identical instruments, measurement protocols, processing and quality assurance schemes, is certainly a viable solution to increase consistency of datasets and make them better applicable to the assessment of satellite data products.

By embracing such a measurement concept, the Ocean Color component of the Aerosol Robotic Network (AERONET-OC) allows the generation of standardized data relevant for the assessment of primary satellite ocean color products (i.e., spectral normalized water-leaving radiance L_{WN} and aerosol optical thickness τ_a) in coastal regions (Zibordi et al., 2009).

This work presents and discusses AERONET-OC optical radiometric data collected at the Gloria site (hereafter GLR) in the Western Black Sea to support satellite ocean color validation activities. Specifically, after a brief introduction to the bio-optical properties of the region and to the in situ measurements from the GLR site, the study focuses on the assessment of satellite primary data products from the Moderate Resolution Imaging Spectroradiometer onboard the Aqua platform (MODIS-A) launched on May 2002 and data from the Visible/Infrared Imager/Radiometer Suite (VIIRS) onboard the Suomi National Polar-orbiting Partnership (NPP) launched on October 2011. The assessment is also extended to the AERONET-OC Acqua Alta Oceanographic Tower site (hereafter AAOT) established in the northern Adriatic Sea in 2002. In fact the long data

OSD
11, 3003–3034, 2014

record and the large bio-optical variability characterizing the AAOT site, provide a term of reference to comprehensively evaluate and discuss GLR results.

2 The measurement site

The Black Sea receives drainage from almost one-third of continental Europe through the Danube, Dniester and Dnieper rivers. The nutrients injected into the basin by these northwestern rivers and the small water exchange with the Mediterranean Sea through the Bosphorus Strait, have strongly influenced the Black Sea biological and bio-geochemical processes during the last decades (e.g., Kideys, 2002; Oguz, 2005). The severe environmental degradation of the basin with almost 90 % of its volume affected by serious anthropogenic pressure, has triggered the need for extended regional investigations. However, the use of satellite ocean color imagery to perform biological and bio-geochemical investigations in the Black Sea has been hindered by the limited statistical representativity of bio-optical algorithms based on a small number of in situ measurements, supporting the generation of high-level satellite data products (Kopelevich et al., 2004; Sancak et al., 2005).

In view of supporting a better exploitation of satellite ocean color data in the Black Sea, since 2006 a number of dedicated bio-optical oceanographic campaigns were performed in the western side of the basin (Zibordi et al., 2011) with the objective of contributing to bio-optical modelling and validation activities (D'Alimonte et al., 2012, 2014; Zibordi et al., 2013). Complementary to ship measurements, since late 2010 an AERONET-OC site was established in the Romanian Shelf southeast of the Danube plume (long. 29.360° E and lat. 44.600° N) to create time-series of in situ reference data for continuous validation of satellite ocean color products.

The site, operated in collaboration with the National Institute for Marine Research and Development "Grigore Antipa" in Constanta, relies on the Gloria platform owned and managed by the Petrom oil company. Due to its location in the northwestern Shelf Region (see Fig. 1), GLR contributes to AERONET-OC globally distributed measure-

OSD
11, 3003–3034, 2014

ments with data generally representing water moderately dominated by sediments and colored dissolved organic matter. However, it is expected that the site may occasionally exhibit unique concentrations of coccolithophores during the summer season and high sediment concentration during seasons affected by high runoff from the Danube.

The Chl *a* climatology of the Black Sea is illustrated in Fig. 1 through maps constructed with MODIS-A data from 2002 to 2010 for the months of January, April, July and October. Chl *a* values clearly indicate different bio-optical regimes for the western Shelf and the open sea regions. In particular, in agreement with previous in situ measurements and satellite observations (Vinogradov et al., 1999; Sorokin, 2002; Kopelevich et al., 2004; McQuatters-Gollop et al., 2008), Chl *a* concentrations exhibit the highest values during winter in the open Black Sea regions while in the western Shelf they show maxima pronounced in late spring-summer and less marked in fall.

Typical values of quantities characterizing optically significant constituents for the Western Black Sea waters, which refer to in situ data collected within the framework of the Bio-Optical mapping of Marine optical Properties (BiOMaP) measurement program (Zibordi et al., 2011), are summarized in Table 1. These values have been determined using measurements from 316 stations performed during 8 oceanographic cruises from 2006 to 2012. The large SD characterizing Chl *a*, is an index of the large variability affecting the western basin.

3 Assessment of satellite data products

The application of GLR data and those from the Acqua Alta Oceanographic Tower (AAOT) to the assessment of satellite ocean color primary products is proposed in the following sections. In view of providing the basis for such an assessment, in situ and satellite data, the criteria applied for the construction of matchups (i.e., pair of in situ and satellite data) and the methodology used for the analysis, are briefly introduced in the following subsections.

3.1 In situ AERONET-OC data

AERONET-OC aims at delivering standardized in situ normalized water-leaving radiance L_{WN} (Zibordi et al., 2009) and aerosol optical thickness τ_a (Smirnov et al., 2000, Holben et al., 1998) through: (i) the use of identical instruments and of a unique measurement protocol; (ii) the calibration of network radiometers by applying a sole method and laboratory; and finally (iii) the reduction and quality control of measurements by using a single processing code.

It is reminded that the processing and quality control are performed in agreement with the scheme presented in Zibordi et al. (2009). This implies the correction of the effects of non-isotropy of the in water light field and surface reflectance following the method proposed by Morel et al. (2002). It is recognized that this method, that was proposed for chlorophyll *a* dominated waters, is certainly challenged in coastal regions. Nevertheless, the related uncertainties are accounted for in the uncertainty budget for L_{WN} (Zibordi et al., 2009).

Data products determined at different center-wavelengths λ in the 412–1020 nm spectral region (nominally, 412, 443, 488, 531, 551, 667, 870 and 1020 nm), are available at three levels of quality control: (i) Level-1.0 derived from complete sequences of in situ measurements; (ii) Level-1.5 obtained after cloud-screening and applying a series of quality tests designed to remove measurements affected by significant environmental perturbations or artifacts; and finally (iii) Level 2.0 comprising fully quality-controlled data generated after post-deployment calibration and check of individual data records. Level 1.0 and Level-1.5 data are accessible in almost real-time through a web interface. Level-2 data products are only accessible after each deployment period lasting approximately 6–12 months. The data analysis included in this study is only based on Level-2 data.

A comprehensive evaluation of uncertainties affecting AERONET-OC L_{WN} was performed for a number of sites exhibiting a variety of water types and different atmospheric aerosols (Gergely and Zibordi, 2014). In the specific case of the GLR site,

OSD
11, 3003–3034, 2014

results indicate mean relative combined uncertainties of 5–10 % in the 412–667 nm spectral region. The corresponding absolute combined uncertainties vary from approximately 0.03 to 0.04 $\mathrm{mW\,cm^{-2}\,\mu m^{-1}\,sr^{-1}}$ between 412 and 551 nm, and exhibit a value of 0.01 $\mathrm{mW\,cm^{-2}\,\mu m^{-1}\,sr^{-1}}$ at 667 nm. In the case of the AAOT site, the relative combined uncertainties are lower than those determined for GLR data and show values of approximately 5 % between 412 and 551 nm, increasing to 7 % at 667 nm. Conversely, the absolute combined uncertainties are slightly larger for the AAOT data in the 412–551 nm region with values varying from 0.04 to 0.06 $\mathrm{mW\,cm^{-2}\,\mu m^{-1}\,sr^{-1}}$, while the value at 667 nm is identical (i.e., 0.01 $\mathrm{mW\,cm^{-2}\,\mu m^{-1}\,sr^{-1}}$). These estimated values account for uncertainties due to: (i) absolute calibration, (ii) change in instrument sensitivity during field deployment; (iii) corrections for the viewing angle geometry and the anisotropy of water and surface light fields; (iv) variability in the input quantities required to determine L_{WN} (e.g., wind speed, surface reflectance, diffuse atmospheric transmittance); and (v) environmental perturbations, which exhibit the largest contribution, due to wave effects and changes in illumination and water masses during measurement sequences. For completeness, it is mentioned that uncertainties of AERONET τ_{a} values are lower than ±0.02 (Eck et al., 1999).

The GLR spectra in Fig. 2 exhibit maxima at 547 nm for 55 % of the cases and at 488 nm for 29 %. Differently, the AAOT L_{WN} spectra have maxima occurring at 488 nm for 80 % of the cases and at 547 nm for 17 % only.

The representativity of the GLR and AAOT L_{WN} spectra with respect to those from different European water types constituting the BiOMaP data set, is evaluated through features indicating shape and amplitude of spectra (Zibordi et al., 2011; D'Alimonte et al., 2012). Specifically, after correcting the GLR and AAOT data for the effects of differences in center-wavelengths with respect to those characterizing the BiOMaP data (i.e., 412, 443, 490, 555 and 665 nm), the spectral shape is represented through the first two components from the Principal Component Analysis (PCA, see Jollife, 1986) of spectra normalized to their values at 555 nm (i.e., $L_{\mathrm{WN}}(\lambda)/L_{\mathrm{WN}}(555)$, with $\lambda = 412$,

OSD
11, 3003–3034, 2014

In situ optical radiometry in the Western Black Sea

G. Zibordi et al.

443, 490 and 670 nm). The amplitude of spectra is simply given by the scaling value $L_{WN}(555)$.

Projections of BiOMaP, GLR and AAOT L_{WN} spectra are displayed in Fig. 3. Circles indicate the projection of single BiOMaP spectra and the axes correspond to the projective directions (i.e., the first two components of PCA, and $L_{WN}(555)$). On the basis of a priori knowledge of regional water types, the blue, red, and green circles indicate oligotrophic and mesotrophic chlorophyll *a* dominated waters, yellow-substance dominated waters, and moderately sediment-dominated waters, respectively. GLR and AAOT data are presented through contour plots from density distributions of projected spectra superimposed to the BiOMaP values. Specifically, the GLR and AAOT L_{WN} projected spectra have been mapped to a uniform grid and the contour lines have then been constructed from the number of occurrences of the grid cells. Each line in Fig. 3 represents a 10 % increment with value varying from 10 % (light yellow) to the maximum value of occurrences (black).

As already evident from the similarities shown by the spectra in Fig. 2, the GLR and AAOT data mapped in Fig. 3 exhibit large areas of overlapping. Ultimately, both GLR and AAOT L_{WN} spectra represent optically complex waters, with GLR data exhibiting a large number of cases overlapping with the Baltic Sea water dominated by colored dissolved organic matter (see the density distribution of the darkest isolines in Fig. 3).

3.2 Satellite data

Match-ups for the GLR and AAOT sites were constructed using MODIS-A data acquired from the Goddard Space Flight Center (GSFC) of the National Aeronautics and Space Administration (NASA) and processed with the SeaWiFS Data Analysis System (SeaDAS) software package version 7.0 (Fu et al., 1998; Gordon and Wang, 1994; Wang et al., 2005). Differently, the VIIRS Level-2 data were acquired as Level-2 from GSFC. Consistently with AERONET-OC data, MODIS-A L_{WN} remote sensing data products at the 412, 443, 488, 531, 547 and 667 nm center-wavelengths, and VI-

IRS data at 410, 443, 486, 551, 671 nm, are corrected for bi-directional effects applying the same scheme.

3.3 Band-shift correction and regional algorithms

Comparisons of in situ and satellite L_{WN} may be affected by differences in center-wavelengths between sensors. This potential source of uncertainty is minimized through the application of specific adjustments factors to the in situ L_{WN} (i.e., band-shift correction) in agreement with the scheme outlined by Zibordi et al. (2006), Mélin and Zibordi (2007) and Zibordi et al. (2009).

In summary, the synthetic value $L_{\mathrm{WN}}(\lambda)$ at the center-wavelength λ is determined from the actual $L_{\mathrm{WN}}(\lambda_0)$ at a near center-wavelength λ_0 assuming ideal 10 nm wide spectral band-widths, from

$$L_{\mathrm{WN}}(\lambda) = L_{\mathrm{WN}}(\lambda_0)\frac{E_0(\lambda)}{E_0(\lambda_0)}\frac{b_{\mathrm{b}}(\lambda)}{a(\lambda)+b_{\mathrm{b}}(\lambda)}\frac{a(\lambda_0)+b_{\mathrm{b}}(\lambda_0)}{b_{\mathrm{b}}(\lambda_0)} \tag{1}$$

where $E_0(\lambda)$ is the extra-atmospheric solar irradiance (Thuillier et al., 2003), $a(\lambda)$ the total water absorption coefficient and $b_{\mathrm{b}}(\lambda)$ the total backscattering coefficient. It is recalled that $a(\lambda)$ is given by the sum of contributions due to particulate matter, $a_{\mathrm{p}}(\lambda)$, (separated into contributions by pigmented, $a_{\mathrm{ph}}(\lambda)$, and non-pigmented, $a_{\mathrm{dp}}(\lambda)$, particles), colored dissolved organic matter $a_{\mathrm{y}}(\lambda)$, and pure seawater, $a_{\mathrm{w}}(\lambda)$. The value of $b_{\mathrm{b}}(\lambda)$ is given by the sum of the backscattering coefficients of particulate matter, $b_{\mathrm{bp}}(\lambda)$, and of pure seawater, $b_{\mathrm{bw}}(\lambda)$.

The relevant spectral input quantities defining $a(\lambda)$ and $b_{\mathrm{b}}(\lambda)$, excluding $a_{\mathrm{w}}(\lambda)$ and $b_{\mathrm{bw}}(\lambda)$, which are known, are iteratively determined using regional algorithms relying on the logarithm of remote sensing reflectance ratios

$$R_{\mathrm{rs}}(\lambda_i,\lambda_j) = \log_{10}[R_{\mathrm{rs}}(\lambda_i)/R_{\mathrm{rs}}(\lambda_j)] \tag{2}$$

OSD
11, 3003–3034, 2014

where the remote sensing reflectance $R_{rs}(\lambda)$ (with $\lambda = \lambda_i, \lambda_j$) is determined from AERONET-OC $L_{WN}(\lambda)$ with

$$R_{rs}(\lambda) = L_{WN}(\lambda)/E_0(\lambda) \tag{3}$$

While site specific algorithms were already provided for the AAOT in a different work (Zibordi et al., 2009), regional algorithms applicable to GLR data have been developed using in situ BiOMaP data from the Western Black Sea.

Following Morel and Maritorena (2001), the spectral values of $a_{ph}(\lambda)$ are estimated from

$$a_{ph}(\lambda) = 0.06 a_c(\lambda) \mathrm{Chl}\ a^{0.65} \tag{4}$$

where $a_c(\lambda)$ is the chlorophyll *a* specific absorption coefficient (Prieur and Sathyendranath, 1981) and Chl *a* is computed from

$$\begin{aligned}\log_{10}(\mathrm{Chl}\ a) = &-0.0661 - 2.8542 R_{rs}(488,547) + 1.1787 R_{rs}^2(488,547) \\ &- 4.8159 R_{rs}^3(488,547)\end{aligned} \tag{5}$$

with coefficients derived from the regression of in situ Chl *a* and $R_{rs}(488,547)$ ratios with determination coefficient $r^2 = 0.88$ and $N = 316$. Equation (5) has been applied to MODIS-A $R_{rs}(\lambda)$ for the determination of the Chl *a* maps presented in Fig. 1.

The estimate of $a_{dp}(\lambda)$ is made through (Yentsch, 1962; Kirk, 1980)

$$a_{dp}(\lambda) = a_{dp}(412) \exp[-S_{dp} \cdot (\lambda - 412)] \tag{6}$$

where $S_{dp} = 0.011\ \mathrm{nm}^{-1}$ (Berthon et al., 2008), and

$$\log_{10} a_{dp}(412) = -0.6941 - 1.259 R_{rs}(488,667) + 0.2714 R_{rs}^2(488,667) \tag{7}$$

with coefficients determined from the regression of in situ $a_{dp}(412)$ and $R_{rs}(488,667)$ ratios with $r^2 = 0.74$ and $N = 316$.

OSD
11, 3003–3034, 2014

Spectral values of $a_y(\lambda)$ are estimated using

$$a_y(\lambda) = a_y(400)\exp[-S_y \cdot (\lambda - 400)] \quad (8)$$

where $S_y = 0.016\,\mathrm{nm}^{-1}$ (Berthon et al., 2008), and

$$\log_{10} a_y(400) = -0.7686 - 0.7737 R_{rs}(412,547) + 0.4909 R_{rs}^2(412,547) \quad (9)$$

with coefficients derived from the regression of in situ $a_y(400)$ and $R_{rs}(412{,}547)$ ratios data with $r^2 = 0.66$ and $N = 316$.

Spectral values of $b_{bp}(\lambda)$ are estimated with

$$b_{bp}(\lambda) = b_{bp}(510) \cdot (\lambda/510)^{-S_{bp}} \quad (10)$$

where $S_{bp} = 1.3$, (Berthon et al., 2008), and

$$\log_{10} b_{bp}(510) = -2.4249 - 1.4155 R_{rs}(490,555) + 0.3347 R_{rs}^2(490,555) \quad (11)$$

with coefficients derived from the regression of in situ $b_{bp}(510)$ and $R_{rs}(412{,}547)$ ratios with $r^2 = 0.61$ and $N = 316$.

Uncertainties in the applied band-shift correction vary with the spectral distance between the target wavelength λ and the actual wavelength λ_0 for which the measurement is available, the spectral region of interest, and the uncertainties of the algorithms applied for the determination of $a(\lambda)$ and $b_b(\lambda)$. In the specific case of MODIS-A matchups, the largest mean corrections applied to GLR AERONET-OC data are of +3.1 % at 443 nm, −1.8 % at 488 nm and +1.3 % at 551 nm. In the case of VIIRS matchups the largest mean corrections are of +2.4 % at 443 nm, −1.9 % at 486 nm and −1.7 % at 410 nm. The uncertainties in the band-shift corrections are then likely to be much smaller than the correction values and thus are assumed to not significantly affect the uncertainty of the corrected data with respect to the original input AERONET-OC data.

OSD
11, 3003–3034, 2014

3.4 Match-up analysis

The comparison of primary satellite and in situ products $\Im$ (i.e., L_{WN} or τ_a) is presented through the average of percent differences, ψ, and average of the absolute percent differences, $|\psi|$, of N match-ups.

The values of ψ are computed through

$$\psi = \frac{1}{N}\sum_{i=1}^{N}\psi_i \tag{12}$$

where i is the match-up index, and ψ_i is

$$\psi_i = 100\frac{\Im^{SAT}(i) - \Im^{PRS}(i)}{\Im^{PRS}(i)} \tag{13}$$

with $\Im^{SAT}$ indicating the quantities computed from satellite observations, and $\Im^{PRS}$ the reference Level-2 AERONET-OC data assumed to have uncertainties much smaller than those affecting the satellite data. The absolute values $|\psi_i|$ are used to compute $|\psi|$ according to

$$|\psi| = \frac{1}{N}\sum_{i=1}^{N}|\psi_i|. \tag{14}$$

The statistical indices ψ and $|\psi|$ are of high immediacy and generically define the bias and dispersion between the compared quantities, respectively. They, however, may not be suitable to consistently report statistical differences for data sets referred to very different ranges of the compared quantity like those characterizing L_{WN} from different water types. Because of this, the root mean square of differences rmsd and the determination coefficient r^2, are also provided as a further aid for the comparison analysis.

OSD
11, 3003–3034, 2014
In situ optical radiometry in the Western Black Sea
G. Zibordi et al.

The MODIS and VIIRS remote sensing products utilized for match-up construction have been obtained from the average of the 3×3 pixel values centered at the measurement site. These averages have been retained when: (i) none of the nine pixels is affected by the standard flags of the SeaDAS processing code (Bailey and Werdell 2006) mainly indicating cloud or sun glint contaminations; (ii) the viewing and sun zenith angles are lower than 60° and 70°, respectively; (iii) the coefficient of variation (ratio of the SD to the mean) of L_{WN} at 547 nm for MODIS or at 551 nm for VIIRS, from the 3×3 image elements centered at the measurement site, is lower than a threshold ξ_L to exclude data affected by a high spatial variability around the sampling point; (iv) the difference between in situ and satellite data sampling time is lower than a threshold Δ_t to exclude matching data potentially affected by significant changes with time in measurement conditions.

The need to have high quality data and additionally a statistically significant number of pairs may lead to conflicting criteria for the construction of a match-up set. Specifically, while a low ξ_L and a narrow Δ_t are expected to satisfy greater quality needs, high ξ_L and wide Δ_t are often required to produce a significant number of match-ups.

Based on previous investigations (Zibordi et al., 2009), the current match-up analysis has been performed by setting $\xi_L \leq 0.2$ and $\Delta_t \leq \pm 2$ h. An assessment of the appropriateness of the selected thresholds for the GLR site has been performed by applying the stricter conditions $\xi_L \leq 0.1$ and $\Delta_t \leq \pm 1$ h. With reference to the values presented in Sect. 3.5, results from the analysis of MODIS-A relying on L_{WN} match-up values at 547 nm has shown a decrease of 16 % (i.e., from 127 to 106) in the number of match-ups and only a slight decrease of 0.1 % in the value of $|\psi|$. The equivalent exercise performed using VIIRS L_{WN} match-ups values at 551 nm has shown a decrease of 37 % (i.e., from 82 to 52) in the number of match-ups and a decrease of 0.3 % in the value of $|\psi|$, thus confirming the suitability of the selected values $\xi_L \leq 0.2$ and $\Delta_t \leq \pm 2$ h, for match-up analysis at GLR. The same criteria have also been applied for the construction of AAOT matchups.

OSD
11, 3003–3034, 2014

3.5 Results from L_{WN} match-ups

The scatter plots of satellite (MODIS-A and VIIRS) vs. in situ GLR matchup data are displayed in Figs. 4 and 5. Results exhibit values of $|\psi|$ decreasing from the blue toward the green and increasing again at the red center-wavelengths. MODIS-A shows values of ψ varying within −5 and +6 % for the center-wavelengths at 443, 488 and 547 nm, which are relevant for the determination of Chl *a*. For the equivalent center-wavelengths, the values of ψ for VIIRS matchups vary from −9 to −6 %.

Excluding data at 412 nm, MODIS-A results are close to those presented with matchups constructed with independent in situ radiometric data collected over a large portion of the western Shelf during successive BiOMaP oceanographic campaigns (Zibordi et al., 2011). The marked differences in ψ observed at 412 nm, i.e., +10 % determined with BiOMaP data instead of −17 % determined with GLR data, are likely due to large differences between in situ and satellite data for some matchups in the lower range of values.

The intra-channel values of ψ in Figs. 4 and 5, indicate that VIIRS systematically underestimates L_{WN} with respect to MODIS-A as already reported in Hlaing et al. (2013). However, the rmsd values are comparable or even slightly smaller for VIIRS (which, assuming identical absolute uncertainties, is in agreement with smaller mean spectral values of L_{WN}). These findings suggest caution in focusing cross-mission comparisons on the sole analysis of relative uncertainties whose results may be largely conditioned by the range of values, the number of samples and their distribution.

In agreement with results from GLR, the statistical analysis from AAOT data more markedly confirms that VIIRS systematically underestimates L_{WN} with respect to MODIS-A. In particular, the values of ψ for MODIS-A displayed in Fig. 6 for the AAOT vary from −3 to −7 % at the center-wavelengths of interest for the determination of Chl *a*. The corresponding values for VIIRS vary from −14 to −17 %. The large ψ values observed between 443 and 551 nm for VIIRS at the AAOT site, may suggest difficulties with the atmospheric correction process more pronounced at the Adriatic Sea site

OSD
11, 3003–3034, 2014

and likely due to a less accurate determination of the aerosol type. It is noted that the large ψ determined at 667 and 671 nm for both MODIS-A and VIIRS at the AAOT, are explained by the very low values of L_{WN} characterizing the site and making questionable the results from the statistical analysis. In agreement with the values of ψ, also the rmsd values for AAOT matchups are significantly larger for VIIRS than for MODIS-A (see Fig. 7). Finally, spectral differences of approximately 0.1 mW cm^{-2} µm^{-1} sr^{-1} clearly differentiate the shape of rmsd determined for the AAOT site with respect to GLR for both VIIRS and MODIS-A at 488 and 547 nm (or equivalent center-wavelengths). These spectral variations are likely explained by different mean shapes and amplitudes of the L_{WN} spectra.

3.6 Results from τ_a match-ups

AERONET-OC offers the unique opportunity to produce values of τ_a at offshore sites likely not contaminated by land sources and this creates almost ideal conditions for the validation of marine aerosol products. Figure 7, that shows MODIS-A validation results for τ_a at GLR for various center-wavelengths, indicates spectrally constant rmsd values of 0.04 while the bias expressed through ψ increases with wavelength from +14 % at 412 nm to +38 % at 667 nm. Comparisons of the Ångström exponent, α, that provides the spectral dependence for τ_a, are shown in the last panel of Fig. 7. The values of α determined at 748 and 869 nm for MODIS-A and at the closest center-wavelengths 667 and 870 nm for AERONET-OC data, indicate a slight overestimate for MODIS-A with a median value of 1.56 vs. 1.35 determined from in situ data.

Equivalent validation results for τ_a at the AAOT (not shown, being already matter of previous independent analysis, e.g., see Zibordi et al., 2013; Mélin et al., 2013) exhibit rmsd decreasing from 0.05 at 412 nm to 0.04 at 667 nm, and values of ψ increasing from +21 to +40 % in the same spectral interval. Additionally, equivalent to GLR, the values of α from MODIS-A at the AAOT exhibit an overestimate with respect to those determined from AERONET-OC data (i.e., 1.61 vs. 1.36). These overestimates are consistent, even though more pronounced, with respect to those described in Mélin et al. (2013).

Results from the analysis of τ_a in the near-infrared and of α across the spectral range of interest (different from the α values plotted in Fig. 7 restricted to the red and near-infrared spectral region), are summarized in Table 2. These results indicate large overestimates for both MODIS-A and VIIRS τ_a in the near-infrared at GLR (i.e., +40 and +54 %, respectively) and at AAOT (+33 and +32 %, respectively), with values of rmsd of 0.03 for both satellite sensors and both sites. The agreement between satellite and in situ determinations of α is quite high with the exception of VIIRS match-ups at GLR, which show underestimated values for VIIRS with median of 1.30 with respect to 1.58 determined from AERONET-OC data. These latter values may suggest a different performance of VIIRS atmospheric correction at the GLR and AAOT sites that may explain the appreciable differences highlighted by the statistical analysis of L_{WN} matchups (see Fig. 6).

3.7 Intra-annual climatology at the GLR and AAOT sites

Considering the relevance of satellite ocean color data for climatological studies in optically complex coastal waters, the intra-annual climatology of the $L_{WN}(547)/L_{WN}(488)$ ratio for MODIS-A or $L_{WN}(551)/L_{WN}(486)$ for VIIRS data, has been investigated at the GLR site using AERONET-OC for comparison. Specifically, Fig. 8 has been constructed using all available data at the time of the analysis. Recalling that, among other optically significant constituents the proposed spectral ratio is largely related to Chl *a*, the annual climatology obtained from the three different data sources exhibits a significant qualitative agreement despite differences in the amount of data and the few years used for the analysis. Specifically, regardless of the large variability of the spectral ratio explained by the expected large inter-annual differences (McQuatters-Gollop et al., 2008), the time-series exhibit an extended maximum in winter increasing during early spring. Secondary maxima occur from late spring and in fall. The succession of maxima can

OSD
11, 3003–3034, 2014

be explained by the specific location of GLR in a region influenced by two seasonal cycles, i.e., that typical of the Shelf and of the open sea (see Sect. 2).

Overall results provide confidence on climatological applications of MODIS-A and VIIRS data in the Black Sea optically complex waters. The analysis also highlights the suitability of AERONET-OC data to explore bio-optical processes by relying on data collected at a small spatial scale.

4 Discussion and conclusions

This work has addressed the applicability of an AERONET-OC site located in the Western Black Sea (i.e., GLR) for the continuous validation of satellite ocean color primary data products (i.e., L_{WN} and τ_a). The analysis has been conducted including data from the AERONET-OC site in the northern Adriatic Sea (i.e., AAOT) often exhibiting water types similar to those observed at GLR.

Results from the assessment of L_{WN} satellite data products at both GLR and AAOT indicate mean relative percent differences ψ with respect to in situ data at the center-wavelengths 443, 488 and 547 nm (or equivalent), varying between −5 and +6 % for MODIS-A and from −6 to −9 % for VIIRS. These reasonable percent differences at the center-wavelengths commonly applied for the determination of Chl *a*, are overwhelmed by negative values of ψ in the range of 10–20 % at 412 nm and between 20–55 % in the red, quantified for both VIIRS and MODIS-A. Cross-mission inter-comparisons based on both GLR and AAOT AERONET-OC data, suggest a systematic underestimate (more pronounced at the AAOT site) of L_{WN} data for VIIRS with respect to MODIS-A.

The analysis of MODIS-A τ_a satellite-derived data at GLR indicates an increase of ψ from +14 % at 412 to +38 % at 667 nm, with spectrally constant rmsd of 0.04. The analysis of τ_a in the near-infrared indicates large overestimates for both MODIS-A and VIIRS τ_a (i.e., +40 and +54 %, respectively) at GLR and (+33 and +32 %, respectively) at AAOT with values of rmsd of 0.03 for both satellite sensors and both sites.

OSD
11, 3003–3034, 2014

The good agreement between satellite and in situ determinations of α in the full spectral region of interest exhibits an exception for VIIRS match-ups at GLR, that show underestimated values for VIIRS with median of 1.30 with respect to 1.58 determined from AERONET-OC data. This result suggests different performances of the VIIRS atmospheric correction at the GLR and AAOT sites.

An interesting feature is offered by the annual climatology of L_{WN} spectral ratios (i.e., $L_{WN}(547)/L_{WN}(488)$, or equivalent) at the GLR site. Specifically, both in situ and satellite-derived data indicate general trends confirming the existence of two different bio-optical regimes, one typical of the open Black Sea, with high Chl *a* values occurring in winter and increasing during early spring, and the other common for the Shelf region exhibiting maxima from late spring and in fall.

The notable high values of ψ determined from the analysis of in situ and satellite matchups of L_{WN} may create concerns on results, especially when considering the 5 % maximum uncertainty target usually included among the objectives of most satellite ocean color missions. However, it must be recognized that such a target commonly refers to oceanic oligotrophic and mesotrophic Chl *a* dominated waters. In the case of coastal regions, uncertainties associated with L_{WN} tend to increase as the atmospheric correction process is challenged by local conditions. Additionally, the decrease of the L_{WN} values toward the blue, due to an increase of absorption by water constituents with respect to oligotrophic and mesotrophic Chl *a* dominated waters, amplifies the relative differences while assuming identical absolute differences. This suggests that when addressing differences between satellite and in situ data, aside statistical indices providing relative values (i.e., in %) of immediate interpretation, it is important to add indices related to absolute differences.

It is finally underlined that the present work proposes new regional bio-optical algorithms for the Western Black Sea applicable for the determination of a number of bio-optical quantities (i.e., Chl *a*, a_{ph}, a_{dp}, a_y) and for corrections minimizing the effect of differences in center-wavelengths between diverse sources of radiometric data (e.g., in situ and satellite).

Acknowledgements. The authors wish to thank NASA OBPG for granting access to the MODIS and VIIRS data. Additional acknowledgments are due to the NASA AERONET-OC team for the effort placed in maintaining the network infrastructure. Acknowledgments are also due to the personnel of the National Institute for Marine Research and Development "Grigore Antipa" in Constanta and to the Petrom oil company, for the continuous support in maintaining the GLR site. Lastly, unconditioned gratitude is expressed to the many scientists and friends who contributed to the logistic, laboratory and field activities essential for the creation of the Black Sea dataset included in BiOMaP.

References

Bailey, S. W. and Werdell, P. J.: A multi-sensor approach for the on-orbit validation of ocean color satellite data products, Remote Sens. Environ., 102, 12–23, 2006.

Behrenfeld, M. J., O'Malley, R. T., Siegel, D. A., McClain, C. R., Sarmiento, J. L., Feldman, G. C., Milligan, A. J., Falkowski, P. G., Letelier, R. M., and Boss, E. S.: Climate-driven trends in contemporary ocean productivity, Nature, 444, 752–755, 2006.

Berthon, J.-F., Mélin, F., and Zibordi, G.: Ocean colour remote sensing of the optically complex European Seas, in: Remote Sensing of the European Seas, edited by: Barale, V. and Gade, M., Springer, Dordrecht, the Netherland, 35–52, 2008.

D'Alimonte, D., Zibordi, G., Berthon, J. F., Canuti, E. and Kajiyama, T.: Performance and applicability of bio-optical algorithms in different European seas, Remote Sens. Environ., 124, 402–412, 2012.

D'Alimonte, D., Zibordi, G., Kajiyama, T., and Berthon, J.-F.: Comparison between MERIS and regional high-level products in European seas, Remote Sens. Environ., 140, 378–395, 2014.

Eck, T. F., Holben, B. N., Reid, J. S., Dubovik, O., Smirnov, A., O'Neill, N. T., Slutsker, I., and Kinne, S.: Wavelength dependence of the optical depth of biomass burning, urban and desert dust aerosols, J. Geophys. Res., 104, 31333–31350, 1999.

Field, C. B., Behrenfeld, M. J., Randerson, J. T., and Falkowski, P.: Primary production of the biosphere: integrating terrestrial and oceanic components, Science, 281, 237–240, 1998.

Fu, G., Baith, K., and McClain, C.: The SeaWiFS Data Analysis System, in: Proceedings of the 4th Pacific Ocean Remote Sensing Conference, Quigdao, China, July 1998, 73–79, 1999.

Gergely, M., and Zibordi, G.: Assessment of AERONET L_{WN} uncertainties, Metrologia 51, 40–47, 2014.

Gordon, H. R. and Wang, M.: Retrieval of water-leaving radiance and aerosol optical thickness over the oceans with SeaWiFS: a preliminary algorithm, Appl. Optics, 33, 443–452, 1994.

Hlaing, S., Harmel, T., Gilerson, A., Foster, R., Weidemann, A., Arnone, R., Wang, M., and Ahmed, S.: Evaluation of the VIIRS ocean color monitoring performance in coastal regions, Remote Sens. Environ., 139, 398–414, 2013.

Holben, B. N., Eck, T. F., Slutsker, I., Tanré, D., Buis, J. P., Setzer, A., Vermote, E., Reagan, J. A., Kaufman, Y. J., Nakajima, T., Lavenu, F., Jankowiak, I., and Smirnov, A.: AERONET – a federated instrument network and data archive for aerosol characterization, Remote Sens. Environ., 66, 1–16, 1998.

Jolliffe, I.: Principal Component Analysis, John Wiley and Sons, Ltd, 2005.

Kideys, A. E.: Fall and rise of the Black Sea ecosystem, Science, 297, 1482–1484, 2002.

Kirk, J. T. O.: Spectral absorption properties of natural waters: contribution of the soluble and particulate fractions of light absorption in some inland waters of south-eastern Australia, Aust. J. Mar. Fresh. Res., 31, 287–296, 1980.

Kopelevich, O. V., Burenkov, V. I., Ershova, S. V., Sheberstov, S. V., and Evdoshenko, M. A.: Application of SeaWiFS data for studying variability of bio-optical characteristics in the Barents, Black and Caspian Seas, Deep-Sea Res. Pt. II, 51, 1063–1091, 2004.

Longhurst, A., Sathyendranath, S., Platt, T., and Caverhill, C.: An estimate of global primary production in the ocean from satellite radiometer data, J. Plankton Res., 17.6, 1245–1271, 1995.

Lohrenz, S. E. and Cai, W.-J.: Satellite ocean color assessment of air–sea fluxes of CO_2 in a river-dominated coastal margin, Geophys. Res. Lett., 33, L01601, doi:10.1029/2005GL023942, 2006.

McQuatters-Gollop, A., Mee, L. D., Raitsos, D. E., and Shapiro, G. I.: Non-linearities, regime shifts and recovery: the recent influence of climate on Black Sea chlorophyll, J. Marine Syst., 74, 649–658, 2008.

Mélin, F. and Zibordi, G.: Optically based technique for producing merged spectra of water-leaving radiances from ocean color remote sensing, Appl. Optics, 46, 3856–3869, 2007.

Mélin, F., Zibordi, G., Carlund, T., Holben, B. N., and Stefan, S.: Validation of SeaWiFS and MODIS Aqua-Terra aerosol products in coastal regions of European marginal seas, Oceanologia, 55, 25–71, 2013.

OSD

11, 3003–3034, 2014

In situ optical radiometry in the Western Black Sea

G. Zibordi et al.

Morel, A. and Maritorena, S.: Bio-optical properties of oceanic waters: a reappraisal, J. Geophys. Res., 106, 7163–7180, 2001.
Morel, A., Antoine, D., and Gentili, B.: Bidirectional reflectance of oceanic waters: accounting for Raman emission and varying particle scattering phase function, Appl. Optics, 41, 6289–6306, 2002.
Oguz, T.: Anthropogenic Forcing, Oceanography, 18, 112–121, 2005.
Platt, T., Fuentes-Yaco, C., and Frank, K. T.: Marine ecology: spring algal bloom and larval fish survival, Nature, 423, 398–399, 2003.
Prieur, L. and Sathyendranath, S.: An optical classification of coastal and oceanic waters based on the specific spectral absorption curves of phytoplankton pigments, dissolved organic matter, and other particulate materials, Limnol. Oceanogr., 46, 1130–1140, 1981.
Sancak, S., Besiktepe, S. T., Yilmaz, A., Lee, M. and Frouin, R.: Evaluation of SeaWiFS chlorophyll-a in the Black and Mediterranean Seas, Int. J. Remote Sens., 26, 2045–2060, 2005.
Smirnov, A., Holben, B. N., Eck, T. F., Dubovik, O., and Slutsker, I.: Cloud screening and quality control algorithms for the AERONET database, Remote Sens. Environ., 73, 337–349, 2000.
Stumpf, R. P.: Applications of satellite ocean color sensors for monitoring and predicting harmful algal blooms, Hum. Ecol. Risk Assess., 7, 1363–1368, 2001.
Sorokin, Y. A.: The Black Sea: ecology and oceanography, in: Biology of Inland Waters, Backhuys, Leiden, the Netherlands, 875 pp., 2002.
Thuillier, G., Hersé, M., Labs, D., Foujols, T., Peetermans, W., Gillotay, D., Simon, P. C., and Mandel, H.: The solar spectral irradiance from 200 to 2400 nm as measured by the SOLSPEC spectrometer from the Atlas and Eureca missions, Sol. Phys., 214, 1–22, 2003.
Vinogradov, M., Shushkina, E., Mikaelyan, A., and Nezlin, N. P.: Temporal (seasonal and interannual) changes of ecosystem of the openwaters of the Black Sea. in: Environmental Degradation of the Black Sea: Challenges and Remedies, edited by: Besiktepe, S. T., Unlüata, U., and Bologa, A. S., Kluwer Academic Publishers, 109–129, 1999.
Wang, M., Knobelspiesse, K. D., and McClain, C. R.: Study of the Sea-viewing Wide Field-of-View Sensor (SeaWiFS) aerosol optical property data over ocean in combination with the ocean color products, J. Geophys. Res., 110, D10S06, doi:10.1029/2004JD004950, 2005.
Ware, D. M. and Thompson, R. E.: Bottom-up ecosystem trophic dynamics determine fish production in the Northeast Pacific, Science, 308, 1280–1284, 2005.

Werdell, P. J. and Bailey, S. W.: An improved in-situ bio-optical data set for ocean color algorithm development and satellite data product validation, Remote Sens. Environ., 98, 122–140, 2005.

Yentsch, C. S.: Measurement of the visible light absorption by particulate matter in the ocean, Limnol. Oceanogr., 7, 207–217, 1962.

Zibordi, G., Mélin, F., and Berthon, J.-F.: Comparison of SeaWiFS, MODIS and MERIS radiometric products at a coastal site, Geophys. Res. Lett., 33, L06617, doi:10.1029/2006GL025778, 2006.

Zibordi, G., Holben, B., Slutsker, I., Giles, D., D'Alimonte, D., Mélin, F., Berthon, J.-F., Vandemark, D., Feng, H., Schuster, G., Fabbri, B. E., Kaitala, S., and Seppälä, J.: AERONET-OC: a network for the validation of Ocean Color primary radiometric products, J. Atmos. Ocean. Tech., 26, 1634–1651, 2009.

Zibordi, G., Berthon, J.-F., Mélin, F., and D'Alimonte, D.: Cross-site consistent in situ measurements for satellite ocean color applications: the BiOMaP radiometric dataset, Remote Sens. Environ., 115, 2104–2115, 2011.

Zibordi, G., Mélin, F., Berthon, J.-F., and Canuti, E.: Assessment of MERIS ocean color data products for European seas, Ocean Sci., 9, 521–533, doi:10.5194/os-9-521-2013, 2013.

OSD

11, 3003–3034, 2014

Table 1. Median (med), mean (avg) and standard deviation (SD) values of optical properties, concentration of constituents and salinity of the Western Black Sea waters (specifically: absorption coefficients of pigmented particles, a_{ph}, non-pigmented particles, a_{dp}, and colored dissolved organic matter, a_y, at 443 nm; backscattering coefficient of particles, b_{bp}, at 443 nm; diffuse attenuation coefficient K_d at 490 nm; concentration of total suspended matter (TSM) and chlorophyll *a* (Chl *a*); salinity, S_w).

Quantity	$a_{ph}(443)$ [m^{-1}]	$a_{dp}(443)$ [m^{-1}]	$a_y(443)$ [m^{-1}]	$b_{bp}(443)$ [m^{-1}]	$K_d(490)$ [m^{-1}]	TSM [$mg\,L^{-1}$]	Chl *a* [$\mu g\,L^{-1}$]	S_w [psu]
med	0.028	0.018	0.106	0.0078	0.116	0.52	0.41	17.01
avg	0.084	0.026	0.129	0.0125	0.185	0.94	1.38	16.05
SD	0.132	0.026	0.071	0.0090	0.204	0.92	2.57	4.47

OSD
11, 3003–3034, 2014

Table 2. Results from the analysis of satellite (SAT) and AERONET-OC (PRS) τ_a match-ups at 869 nm for MODIS-A or 862 nm for VIIRS, at the GLR and AAOT sites. N indicates the number of match-ups, rmsd is the root mean of squared differences, $|\psi|$ is the mean of absolute percent differences while ψ is the mean of percent differences, r^2 is the determination coefficient. The symbols m^{SAT}, m^{PRS}, σ^{SAT} and σ^{PRS} indicate the median and SD, respectively, of the α values determined for satellite data (i.e., SAT) with τ_a at 443 and 869 nm for MODIS-A, with τ_a from 443 to 862 nm for VIIRS, and at equivalent wavelengths for AERONET-OC data (i.e., PRS).

	N	rmsd	$\|\psi\|$	ψ	r^2	$m^{SAT}(\sigma^{SAT})$	$m^{PRS}(\sigma^{PRS})$
MODIS-A at GLR	127	0.03	48	+40	0.50	1.58 (0.41)	1.60 (0.32)
MODIS-A at AAOT	759	0.03	43	+33	0.57	1.61 (0.40)	1.55 (0.39)
VIIRS at GLR	82	0.03	59	+54	0.64	1.30 (0.35)	1.58 (0.41)
VIIR at AAOT	95	0.03	43	+32	0.71	1.39 (0.32)	1.35 (0.50)

OSD
11, 3003–3034, 2014

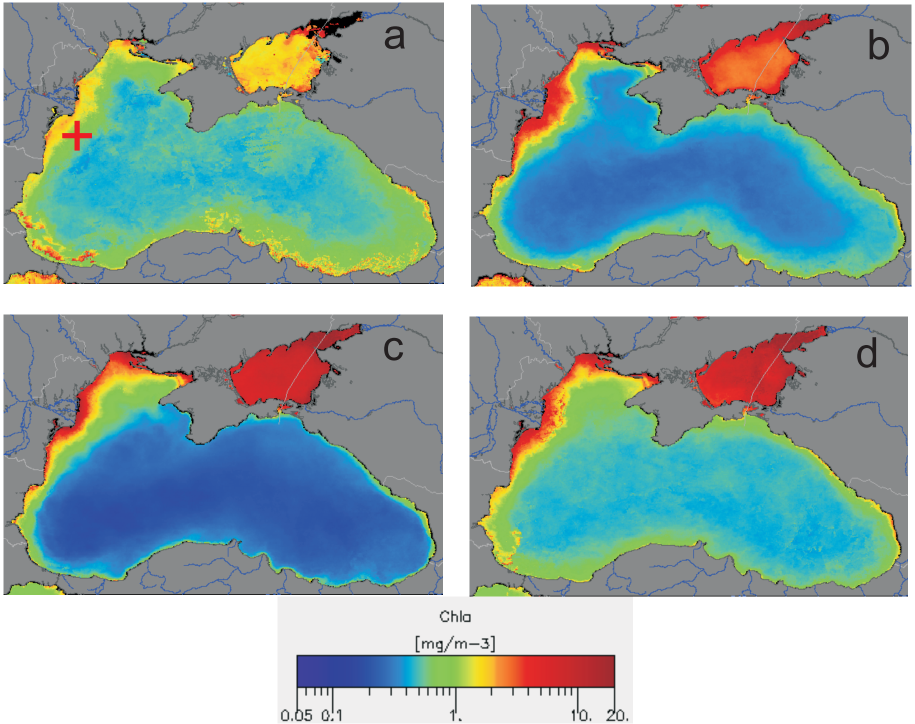

Figure 1. Monthly climatology maps of Chl *a* for the Black Sea (**a**: January; **b**: April; **c**: July; **d**: October) obtained from the application of a regional bio-optical algorithm (see Sect. 3.3 for details) applied to MODIS-A. The red symbol "+" on panel **(a)**, indicates the location of GLR.

OSD
11, 3003–3034, 2014

In situ optical radiometry in the Western Black Sea

G. Zibordi et al.

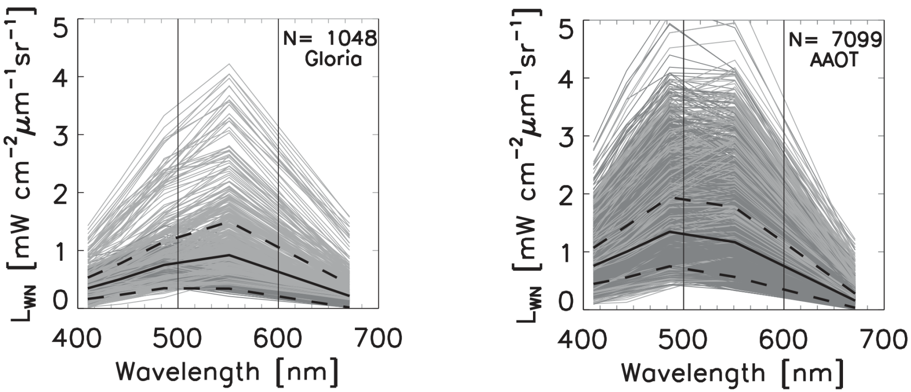

Figure 2. AERONET-OC Level-2 L_{WN} spectra from the GLR and AAOT sites. The thick black-line indicates mean values, while the thick dashed lines indicate ±1 SD.

OSD
11, 3003–3034, 2014

OSD
11, 3003–3034, 2014

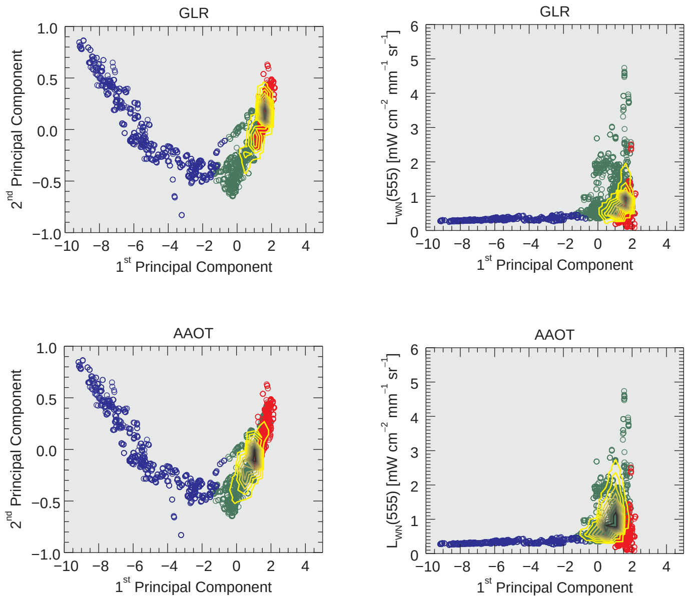

Figure 3. Maps of AERONET-OC L_{WN} spectra from GLR (upper panels) and AAOT (lower panels) with the first two components of PCA applied to $L_{WN}(\lambda)/L_{WN}(555)$ (left panels) and $L_{WN}(555)$ vs. the first PCA component (right panels). While the isolines refer to the density distribution of AERONET-OC L_{WN} from GLR or AAOT sites (indicating 10 % increments from light yellow to black), the circles refer to different water types (see Zibordi et al., 2011): blue for oligotrophic and mesotrophic chlorophyll *a* dominated waters; red for yellow-substance dominated waters; green for a number of optically complex waters likely expected to be moderately sediment dominated.

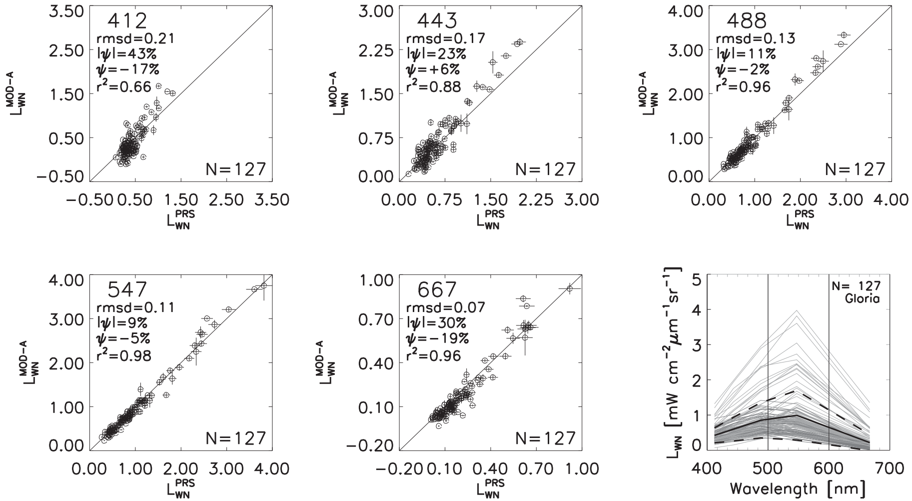

Figure 4. Scatter plots of MODIS-A (MOD-A) vs. AERONET-OC (PRS) L_{WN} match-up values at selected center-wavelengths for the GLR site. N indicates the number of match-ups, L_{WN} and rmsd are in units of $mW\,cm^{-2}\,\mu m^{-1}\,sr^{-1}$, $|\psi|$ is the mean of absolute percent differences while ψ is the mean of percent differences, and r^2 is the determination coefficient. The right panel in the second row displays the AERONET-OC L_{WN} spectra utilized to construct match-ups.

OSD
11, 3003–3034, 2014

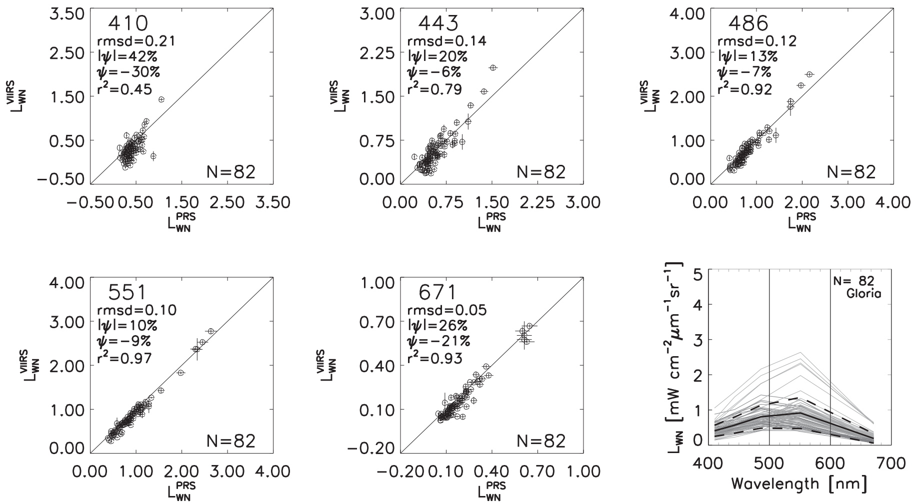

Figure 5. As in Fig. 4, but for VIIRS match-ups at GLR.

OSD
11, 3003–3034, 2014

In situ optical radiometry in the Western Black Sea

G. Zibordi et al.

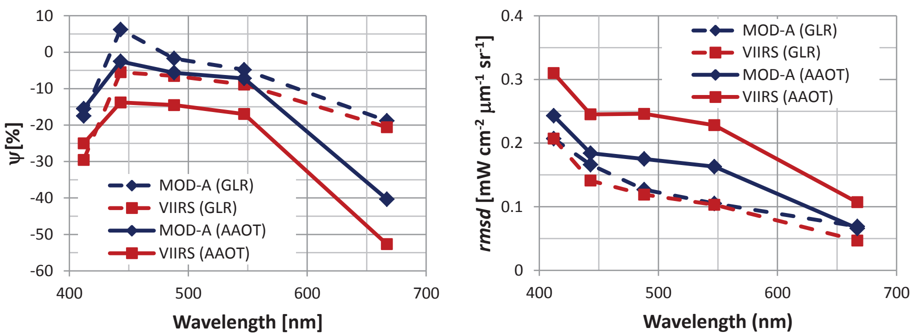

Figure 6. Values of ψ (left panel) and rmsd (right panel) for MODIS-A and VIIRS matchups for the GLR and AAOT sites.

OSD
11, 3003–3034, 2014

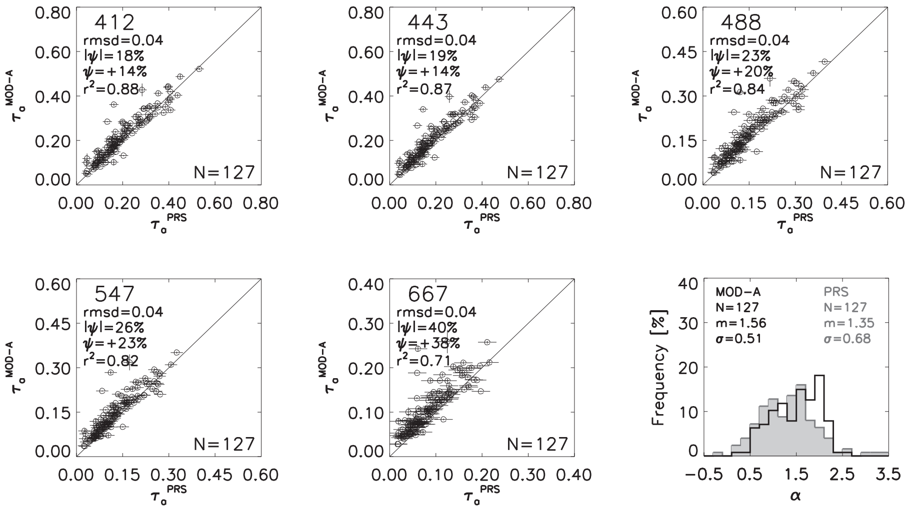

Figure 7. Scatter plot of MODIS-A (MOD-A) vs. AERONET-OC (PRS) τ_a at selected center-wavelengths for the GLR site. N indicates the number of match-ups, τ_a and rmsd are dimensionless, $|\psi|$ is the mean of absolute percent differences while ψ is the mean of percent differences, and r^2 is the determination coefficient. The right panel in the second row displays frequency distributions of α determined with τ_a at 748 and 869 nm for MODIS-A, and 667 and 870 nm for PRS. The black characters and empty bars in the frequency distribution plot, indicate results from the analysis of MODIS-A data while the grey characters and the solid bars indicate results from the analysis of AERONET-OC data (m is the median and σ the SD).

OSD
11, 3003–3034, 2014

In situ optical radiometry in the Western Black Sea

G. Zibordi et al.

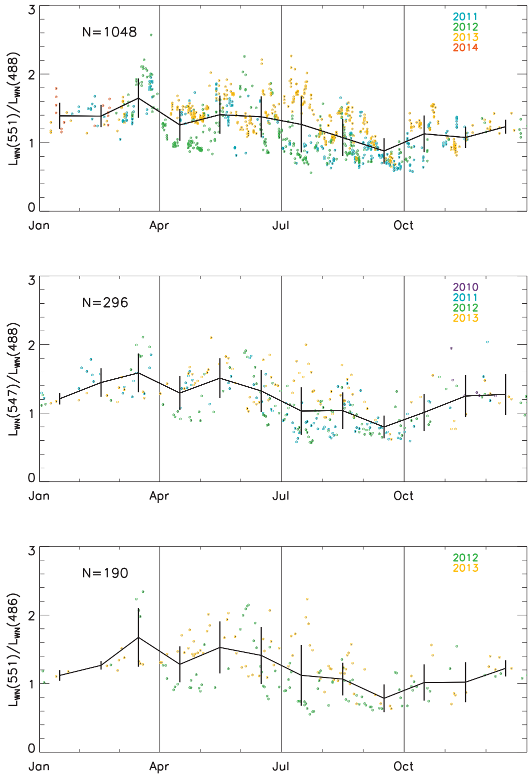

Figure 8. Annual climatology at GLR for the band-ratios L_{WN} (551)/L_{WN}(488) for AERONET-OC (upper panel), L_{WN} (547)/L_{WN}(488) for MODIS-A (central panel) data, and L_{WN} (551)/L_{WN}(486) for VIIRS (lower panel), determined with all available data for the period 2010–2014. The thick black line indicates monthly averages while vertical bars indicate ±1 SD. *N* is the number of data.

OSD
11, 3003–3034, 2014